Lipid-Binding Studies of Human Apolipoprotein A-I and Its Terminally Truncated Mutants†

Yiling Fang, Olga Gursky, and David Atkinson*

Department of Physiology and Biophysics, Boston University School of Medicine, 715 Albany Street, Boston, Massachusetts 02118

Received August 6, 2003; Revised Manuscript Received September 18, 2003

ABSTRACT: Apolipoprotein A-I (apoA-I, 243 amino acids) is the major protein of high-density lipoproteins (HDL) that plays an important structural and functional role in lipid transport and metabolism. The central region of apoA-I (residues 60−183) is predicted to contain exclusively amphipathic α-helices formed from tandem 22-mer sequence repeats. To analyze the lipid-binding properties of this core domain, four terminally truncated mutants of apoA-I, Δ(1−41), Δ(1−59), Δ(1−41,185−243), and Δ(1−59,185−243), were expressed in baculovirus infected Sf-9 cells. The effects of mutations on the ability of apoA-I to form bilayer disk complexes with dimyristoyl phosphatidylcholine (DMPC) that resemble nascent HDL were analyzed by density gradient ultracentrifugation and electron microscopy (EM). The N-terminal deletion mutants, Δ(1−41) and Δ(1−59), showed altered lipid-binding ability as compared to plasma and wild-type apoA-I, and in the double deletion mutants, Δ(1−41, 185−243) and Δ(1−59, 185−243), the lipid binding was abolished. Thermal unfolding of variant apoA-I/DMPC complexes monitored by circular dichroism (CD) showed hysteresis and a shift in the melting curves by about −12 °C upon reduction in the heating rate from 1.0 to 0.067 K/min. This indicates an irreversible kinetically controlled transition with a high activation energy $E_a = 60 \pm 5$ kcal/mol. CD and EM studies of the apoA-I/DMPC complexes at different pH demonstrated that changes in the net charge or in the charge distribution on the apoA-I molecule have critical effects on the conformation and lipid-binding ability of the protein.

Lipoproteins are assemblies of lipids and specific proteins that mainly originate from the liver and the intestine. The major function of lipoproteins is to transport water-insoluble lipids throughout the body. The high-density lipoprotein (HDL)[1] system is comprised of a heterogeneous population of relatively small and dense particles. Their diameters range from 80 to 200 Å, and the densities are between 1.063 and 1.21 g/cm^3 (*1*). The major protein component of HDL is apolipoprotein A-I (apoA-I, 243 amino acids, 28 kD). The major role of HDL is to pick up free cholesterol that is released into the plasma from dying cells and from membranes undergoing turnover. There is a large body of experimental evidence to suggest that augmenting HDL and/or apoA-I can have significant vascular protective effects ranging from prevention to stabilization and regression of atherosclerosis (*2*). This anti-antherogenic function makes HDL a subject of intensive structural and functional studies.

HDL can mainly exist in two different morphologies during metabolism: (a) nascent discoidal particles, with polar lipids in a bilayer conformation and proteins at the circumference of the disk and (b) microemulsion particles, with apopolar cores of cholesteryl esters and triglycerides and polar coats of phospholipids, cholesterol, and proteins (*3*). The conformation of apoA-I on HDL is crucial to HDL functions such as lipid and cholesterol binding, lecithin cholesterol acyltransferase (LCAT) activation, cholesterol ester transfer protein (CETP) binding, SR-BI receptor recognition, and ABC-A1 interaction (*4*).

The secondary structure of apoA-I is dictated by a series of 22- and 11-mer amphipathic α-helices punctuated by prolines (*5*). ApoA-I binds to lipid via the hydrophobic face of the helices. Since native HDL are very heterogeneous, the interaction between apoA-I and lipid has been studied mainly on reconstituted HDL (*6*, *7*). In vitro, the surfactant-like action of apoA-I on multilamellar liposomes or unilamellar vesicles of DMPC to produce HDL-like particles has been well-studied (*8*). The nature and the size of the apoA-I/DMPC complexes depend on the DMPC to apoA-I ratio, ranging from vesicles (1000:1) to large discoidal complexes (300:1) and small discoidal complexes (<100:1). The large and small disks contain three and two apoA-I molecules per particle, respectively.

It has been generally agreed that residues 185−243 play an essential role in lipid binding (*9*). Important individual residues involved in initial lipid binding include carboxyl-terminal hydrophobic residues (*10*) as well as Glu 235 (*11*); point mutations and deletions of these residues lead to a significantly decreased lipid-binding ability. Studies of synthetic peptides (*12*) and deletion mutants (*13*) have shown

† This work was supported by Grants POHL26335 and HL48739 from the National Institute of Health.

* To whom correspondence should be addressed. Phone: (617) 638-4015. Fax: (617) 638-4041. E-mail: atkinson@bu.edu.

[1] Abbreviations: apo, apolipoprotein; CD, circular dichroism; EM, electron microscopy; HDL, high-density lipoprotein; DMPC, dimyristoyl phosphatidylcholine; LCAT, lecithin cholesterol acyltransferase; CETP, cholesterol ester transfer protein; ABC-A1, ATP-binding cassette transporter 1; SR-BI, scavenger receptor class B type I; CSP, consensus sequence peptide; RSP, real sequence peptide; SDS−PAGE, sodium dodecyl sulfate−polyacrylamide gel electrophoresis.

10.1021/bi0354031 CCC: $25.00
Published on Web 10/24/2003

that residues 44−65 and 100−121 may be also involved in lipid binding (*14*).

To map the lipid-binding regions in apoA-I (especially the terminal regions), we designed a series of N- and C-terminal truncated mutants Δ(1−41), Δ(1−59), Δ(1−41, 185−243), and Δ(1−59, 185−243). In previous studies, we have documented the conformation and thermal stability of these mutants in solution at different pH values (*15*). In the current work, the mutants were studied for their ability to bind DMPC under different pH conditions. We also investigated the thermal stability of plasma apoA-I/DMPC complexes via circular dichroism and determined the activation energy for the disk denaturation.

MATERIALS AND METHODS

Protein Expression and Purification. The N-terminal deletion mutants, Δ(1−41) and Δ(1−59), and the double N- and C-terminal deletion mutants, Δ(1−41, 185−243) and Δ(1−59, 185−243), were expressed as His-tagged proteins in insect cell line Sf-9 as described before (*16*). The cells were sonicated, and the proteins in the supernatant were purified by using Ni-nitrilotriacetic acid (Ni-NTA) resin from Qiagen Inc. After purification, the amino terminal 6 × His tag, and the additional 24 residues were removed by tobacco-etched viral (rTEV) protease (also His-tagged) as described before (*15*). The purified apoA-I was analyzed by 12.5% SDS−PAGE, and the concentration was determined by Lowry assay (*17*). The proteins obtained from Sf-9 cells have additional Gly-Ala-Met-Gly-Ser- at the N-terminus that results from the residual rTEV protease site.

Dimyristoyl Phosphatidyl Choline Binding. The reconstitution of the apoA-I/DMPC discoidal complexes that resemble nascent HDL was carried out using the various apoA-I forms. A total of 1.0 mL of lipid (6 μL of ^{14}C-DPPC of 0.05 mCi/mL (NEN Life Science Products, Inc. Boston, MA) in 20 mL of DMPC of 1.036 mg/mL) was aliquoted into a 20 mL glass vial and dried under nitrogen. It was then further dried on the lyophilizer for 15 min. A total of 0.9 mL of sodium phosphate buffer (PBS) was added, and liposomes were made by vortexing vigorously until turbid. ApoA-I was added to the liposomes (PBS was added to the control vial). The amounts of proteins added were ∼0.5 mg for apoA-I variants at pH 7.8 and ∼0.1 mg for those at pH 4.7 because of the limited protein solubility at low pH. The vials were sealed and placed in a shaking water bath at 24 °C overnight. The density of the samples was adjusted to 1.2 g/cm^3 using solid KBr; the samples were then transferred to 5 mL SW-55 Ultraclear (Beckman) tubes. The samples were overlaid with 1.065 g/cm^3 KBr. The tubes were balanced and spun at 50 000 rpm, 15 °C, for 20 h.

After spinning, 25 aliquots of 200 μL each were removed from the surface of the solution. The refractive index of the blank for each fraction was measured by refractometry. A total of 20 μL of each sample fraction was assessed by a Lowry assay (*17*) to locate the positions of the protein component in the apoA-I/DMPC complexes and the free protein. The positions of the lipid component in the complexes and the free lipid were located via scintillation counting.

Electron Microscopy of ApoA-I/DMPC Complexes. ApoA-I/DMPC complexes were imaged by electron microscopy using the negative staining technique. A 4 μL aliquot of sample was applied to a glow-discharged, Formvar-coated, 300 mesh copper grid for 5 min. After blotting extra fluid, the sample was stained with 4 μL of 1% sodium phosphotungstate (negative stain) of appropriate pH for 10 s. Samples were observed on the CM12 electron microscope (Philips Electron Optics, Eindhoven, The Netherlands). Fields of interest were photographed on SO163 film with 1.00 s exposure time, at 45 000 magnification. Films were developed in D19 and scanned on an EverSmart Supreme Scanner (CreoScitex Corp., Vancouver, Canada).

Circular Dichroism Spectroscopy. The CD spectra were measured with an upgraded Aviv 62DS spectropolarimeter equipped with thermoelectric temperature control (Aviv Associates, Lakewood, NJ). Far-UV CD spectra (185−250 nm) were recorded from protein solutions of 0.06−0.10 mg/mL concentrations in 10 mM phosphate buffer (pH 4.7−7.8) placed in 1−2 mm quartz cuvettes. The spectra were recorded every 1 nm, with 15−30 s accumulation time per data point, and averaged over three to five runs. Thermal unfolding and refolding of the protein helical structure was monitored at 222 nm upon heating and cooling between 5 and 95 °C at a rate from 0.067 to 1.0 K/min. All CD experiments were repeated three to four times to ensure reproducibility. After buffer baseline subtraction, the CD data were normalized to protein concentration and are expressed as molar residue ellipticity, [θ]. The values of [θ] were independent of the protein concentrations in the range explored (0.06−0.1 mg/mL). ORIGIN software (Microcal, Amherst, MA) was used for the CD data display and analysis.

Kinetic Analysis of the CD Data. In the absence of well-defined pre- or post-transitional baselines, the apparent melting temperature T_m of the protein/lipid complexes can be determined from the peak position in the first derivative of a heating curve, $d[\theta_{222}(T)]/dT$ (*18*). For a reversible thermal transition, $T_m = T_{1/2}$, where $T_{1/2}$ is the temperature at which 50% of the total CD signal change is observed.

The activation energy (enthalpy) E_a for the irreversible thermal denaturation of the apoA-I/DMPC disks was determined from the heating rate dependence of the apparent melting temperature T_m. According to the Lumry−Eyring model of an irreversible transition, the effect of scan rate υ on T_m is related to E_a as (*19*)

$$\ln(\upsilon/T_m^2) = \text{const} - E_a/RT_m$$

where υ is the heating rate, and $R = 1.987$ cal/mol is the universal gas constant.

If $E_a(T) = \text{const}$, the plot $\ln(\upsilon/T_m^2)$ versus $1/T_m$ is linear with a slope $-E_a/R$. In this paper, the value of E_a for the apoA-I/DMPC complex was determined from such a plot using T_m values determined from the melting curves recorded at different scan rates υ from 0.067 to 1.0 K/min.

RESULTS

Lipid-Binding Properties of Variant ApoA-I Forms. Reconstitution of apoA-I/DMPC complexes was carried out using variant apo A-I forms as described in the Materials and Methods. The complexes were isolated by centrifugation based on the flotation density of plasma apoA-I/DMPC complexes at $d = 1.10$ g/cm^3. The results of the lipid/protein distribution along the density gradient at pH 7.8 are shown in Figure 1.

Table 1: Size and Stoichiometry of Variant ApoA-I/DMPC Complexes

	Plasma					WT	Δ(1−41)	Δ(1−59)
pH	7.8	6.5	6.0	5.5	4.7	7.8	7.8	7.8
diameter[a] (Å)	114[b]	116	115	118	152	116	111	111
DMPC:ApoA-1 ratio								
mass[c]	4.1					2.0	1.6	2.1
molar[c]	170					85	50	50

[a] All the dimensions shown in the table were the averages of the measurements on 150 to ∼250 disks. The thickness of the disks was 55 ± 2 Å for all complexes. [b] ±2 Å. [c] 5−10% error. Ratios were calculated on the data obtained from ultracentrifugation experiments shown in Figure 1 at density ∼1.10 g/cm^3. The dimensions were measured on the disks shown in Figures 2 and 4.

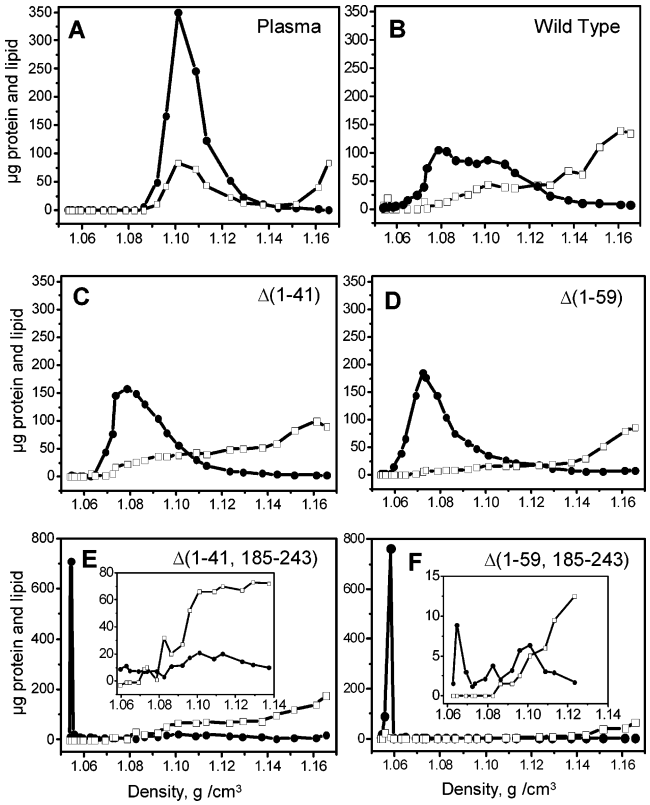

FIGURE 1: Density gradient distribution of variant apoA-I forms binding to DMPC. The density distribution was determined by density gradient centrifugation and plotted in Origin software. □: The amount of apoA-I at each density and ●: the amount of DMPC at each density. Insets in panels E and F: enlargement of density range 1.06−1.14 g/cm^3 showing the amount of protein and DMPC at each density.

Plasma apoA-I bound DMPC very efficiently; it cleared the turbid DMPC dispersion very quickly (less than 5 min). The centrifugation results (Figure 1A) showed a very well-defined peak of both protein and lipid at a density ∼1.10−1.15 g/cm^3, where the apoA-I/DMPC complexes were located. Wild-Type apoA-I also bound to DMPC and formed complexes, as seen in Figure 1B. However, the binding ability of wild-type apoA-I differed from that of plasma apoA-I, as indicated by the slower clearance of the turbid DMPC vesicles (about 15−30 min). Furthermore, the peaks around density 1.10 g/cm^3 in both lipid and wild-type protein were broad, and the lipid showed an additional peak at d = 1.08 g/cm^3, indicating either some unbound DMPC or protein-bound complexes at a density lower than 1.10 g/cm^3 (EM analysis of this sample did not detect any such disks, data not shown). In addition, free protein was detected at the bottom of the gradient.

All mutant proteins showed poor DMPC-binding ability as compared to plasma and wild-type apoA-I. The N-terminal deletions Δ(1−41) and Δ(1−59) cleared the turbid DMPC dispersion after overnight incubation. However, the double deletion mutants Δ(1−41, 185−243) and Δ(1−59, 185−243) never cleared the DMPC dispersion. After the centrifugation, there was a visible layer of free lipid in all tubes containing the mutants. A small amount of free lipid was observed for the N-terminal deletions and a larger amount for the double deletions. Δ(1−41)/DMPC (Figure 1C) and Δ(1−59)/DMPC (Figure 1D) both had a lipid peak at around d = 1.08 g/cm^3 and no obvious peak but a detectable amount of lipid and protein at d = 1.10 g/cm^3. Δ(1−41, 185−243)/DMPC and Δ(1−59, 185−243)/DMPC (Figure 1E,F, respectively) showed a very sharp peak at a density between 1.05 and 1.06 g/cm^3, where DMPC liposomes were located. Most of the protein was at the bottom of the tubes (density > 1.14 g/cm^3) as free protein. There was a little protein and lipid at d = 1.10 g/cm^3, but they were only barely detectable. The lipid/protein ratios for variant apoA-I/DMPC complexes at d = 1.10 g/cm^3 were calculated and are listed in Table 1. The ratios are different for different forms of apoA-I, indicating different lipid/protein composition of the disks.

Electron Microscopic Studies on the ApoA-I/DMPC Complexes. ApoA-I/DMPC complexes prepared with variant apoA-I forms were observed by electron microscopy using the negative staining technique as described in the Materials and Methods. Fractions of density ∼1.10 g/cm^3 of plasma apoA-I/DMPC and all odd-numbered fractions of the 25 fractions of the wild type and the mutant proteins were visualized by EM.

Figure 2A shows an electron micrograph of plasma apoA-I/DMPC complexes with a density of 1.10 g/cm^3. Nearly all the apoA-I was bound to the lipid to form disks. In the negative staining process, most disks stacked on edge and formed numerous stacks of disks with uniform size. The measurement of these disks gave an average thickness of ∼55 Å and diameter of 110 Å (Table 1).

The EM micrographs of the complexes formed by the wild type and the N-terminal deletion mutants Δ(1−41) and Δ(1−59) with DMPC showed that the complexes located at density ∼1.10 g/cm^3 also exhibited discoidal morphology (Figure 2B−D). However, the disk dimensions of the mutant/DMPC complexes were different from those of plasma and wild-type apoA-I (Table 1). EM micrographs of the fractions at other densities did not show obvious discoidal complexes. This indicates that the lipid or the protein density peaks that were not located at 1.10 g/cm^3 (e.g., the peaks centering around 1.07−1.08 g/cm^3 in Figure 1C,D) did not contain any significant amount of apoA-I/DMPC disks. The double deletion mutants Δ(1−41, 185−243) or Δ(1−59, 185−243)

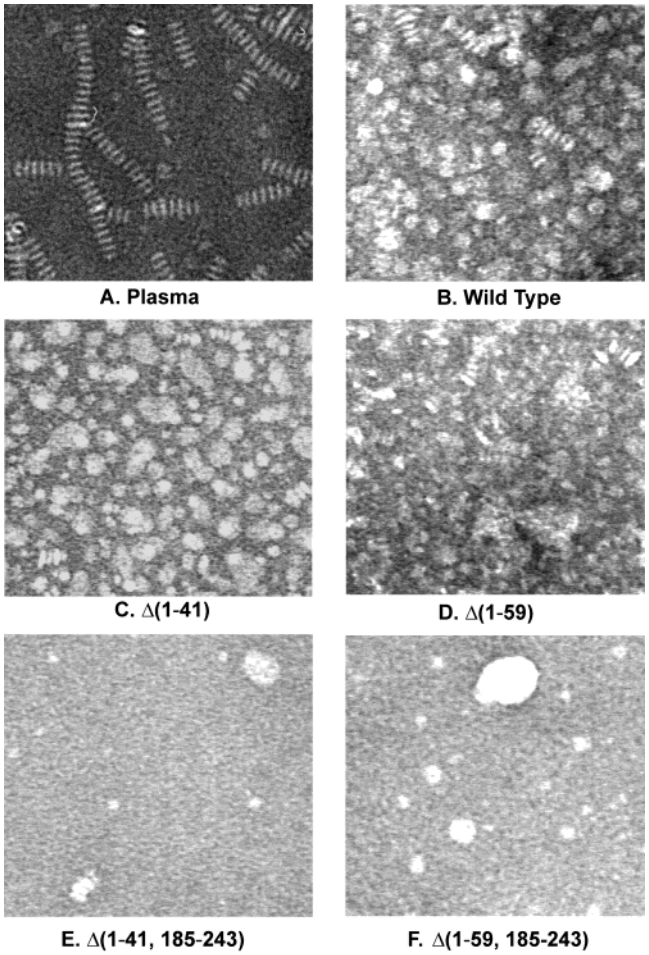

FIGURE 2: Negative staining electron micrographs of variant apoA-I/DMPC complexes. The samples were taken from the fractions of $d = 1.10$ g/cm^3 after ultracentrifugation, where the density of the plasma apoA-I/DMPC disk is located.

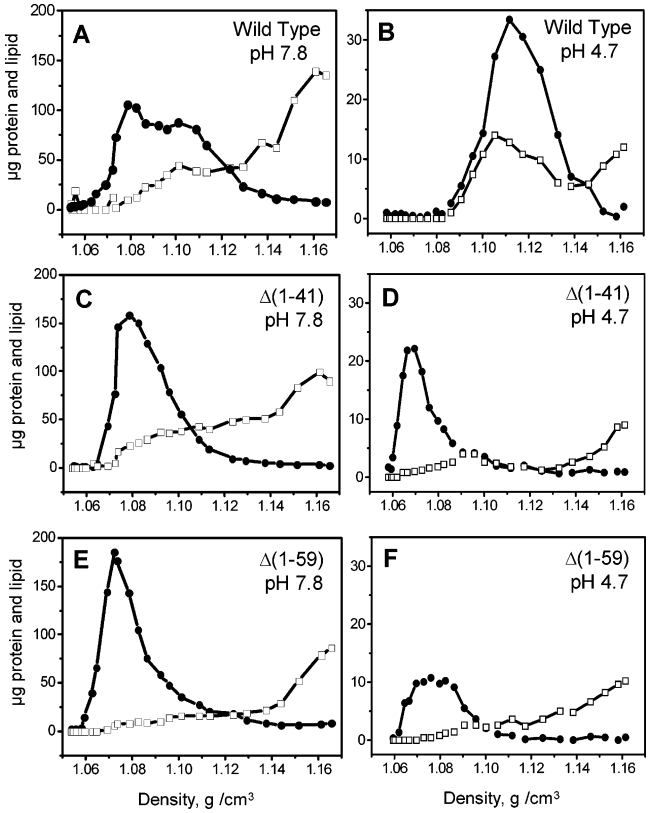

FIGURE 3: Density gradient distribution of variant apoA-I forms binding to DMPC at different pH values. The complexes were initially made at different pH values, and density distribution was determined by density gradient centrifugation. The amounts of proteins added were ~0.5 mg for apoA-I variants at pH 7.8 and ~0.1 mg for those at pH 4.7. □: The amount of apoA-I at each density and ●: the amount of DMPC at each density.

bound DMPC very poorly; hardly any disks were detected for either mutant (Figure 2E−F). These results suggest the importance of both the N-terminal 1−41 segment, and especially, the C-terminal 185−243 segment for the lipid binding by apoA-I.

Effect of pH on ApoA-I/DMPC Complex Formation. As reported earlier, a reduction in pH from 7.8 to 4.7 resulted in an increase in the α-helical content and the unfolding cooperativity of terminally truncated apoA-I variants in solution (*15*). In this work, we studied the lipid-binding properties of these mutants at different pH. Both the protein solution and DMPC suspension were prepared at pH 4.7. For wild-type apoA-I, the peaks of the protein and lipid both became better defined as compared to those at pH 7.8 (Figure 3A,B). The reduction in pH from 7.8 to 4.7 also led to the appearance of a small protein peak at around $d = 1.10$ g/cm^3 for Δ(1−41) and Δ(1−59) (Figure 3C,D).

The apoA-I/DMPC complexes were also made at pH 7.8 based on the ratio in Table 1 and were subsequently dialyzed against 10 mM PBS of a series of pH 7.0, 6.5, 6.0, 5.5, and 4.7. A portion of the sample was taken at each pH for EM analysis. EM micrographs of plasma apoA-I/DMPC disks at different pH (Figure 4, Table 1) showed that at pH 7.8 and 7.0, the size of the disks and stacks appeared very similar. When the pH decreased to 6.5, the stacks became shorter, and this change progressed as the pH further decreased, suggesting a progressive reduction in the concentration of the discoidal complexes. During the dialysis, a white precipitate was observed at pH 6.5, indicating partial protein−lipid dissociation. At pH 6.0, DMPC vesicles emerged, and at pH 4.7, there were barely any disk stacks detected. Wild type and mutant proteins showed a similar trend, that is, a gradual reduction in the disk concentration upon reduction in pH. However, the proteins precipitated at low pH, resulting in a very low concentration of disks (data not shown).

Effects of DMPC Binding on the Secondary Structure and Thermal Unfolding of Variant ApoA-I. The secondary structure and thermal stability of apoA-I and the N-terminal deletion mutants on DMPC disks (fractions at density ~1.10 g/cm3) were analyzed by CD spectroscopy. Far-UV CD spectra at 25 °C of variant apoA-I forms free in solution (Figure 5, open squares) and in discoidal complexes with DMPC (Figure 5, solid circles) showed an increase in the protein α-helical content upon DMPC binding that is summarized in Table 2. This increase constituted about 5% in plasma, 10% in wild type and Δ(1−59), and nearly 25% in Δ(1−41).

The thermal unfolding and refolding curves of the variant forms of apoA-I on DMPC disks were monitored by CD at 222 nm, [$\theta_{222}(T)$], upon heating and cooling from 5 to 95 °C. The results showed remarkable differences from the unfolding data of the lipid-free protein (insets in Figure 5A−D). At a scan rate of $\upsilon = 1.0$ K/min, the thermal unfolding

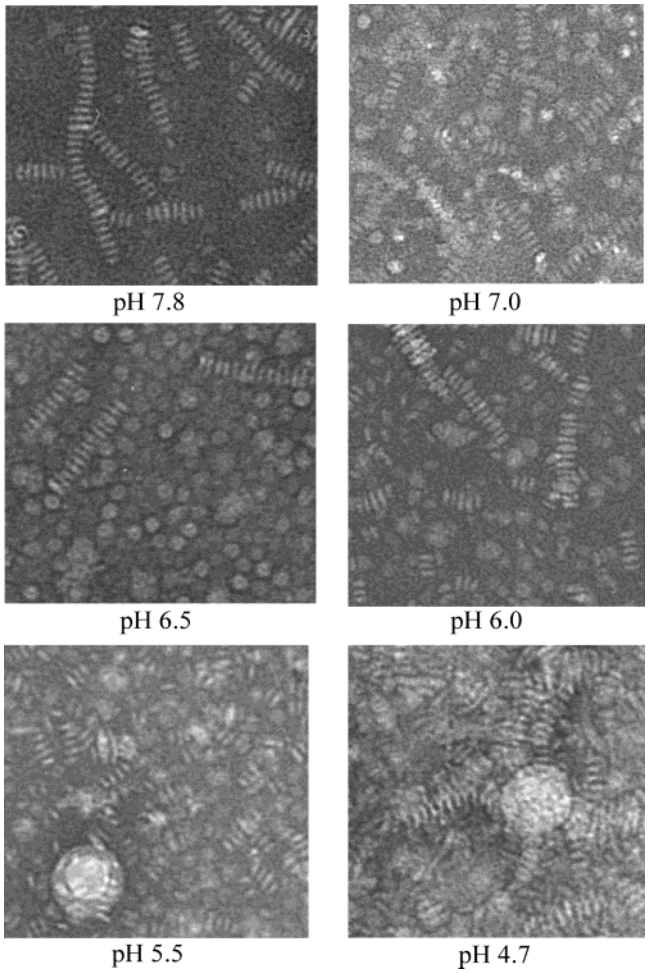

FIGURE 4: Negative staining electron micrographs of plasma apoA-I/DMPC complexes at different pH values. The complexes were initially made at pH 7.8 based on the ratio listed in Table 1 and then dialyzed against 10 mM PBS of a different pH. An aliquot was taken at the end of each dialysis for EM observation.

and refolding curves of the lipid-free apoA-I largely overlapped (open squares in Figure 5A, Figure 6A) which, together with a complete superimposition of the unfolding curves of lipid-free apoA-I recorded at different heating rates (*15*), indicated a reversible thermal transition (*19*).

In contrast to lipid-free apoA-I, the thermal transition of apoA-I on DMPC disks at $\upsilon = 1.0$ K/min was irreversible (solid circles), as indicated by the hysteresis and by a large reduction in the CD signal at 25 °C prior to and following the heating to 95 °C. In plasma apoA-I/DMPC complexes, the refolding curve was shifted to lower temperature by about 35 °C as compared to the unfolding curve (Figure 5A, inset). A similar discrepancy between the heating and the cooling curves was observed in the DMPC disks containing wild type and mutant apoA-I (Figure 5B−D, insets). Similarly, a hysteresis has been documented in the thermal unfolding of other apolipoprotein complexes with DMPC, such as apoC-I (*20*), a 44-residue consensus sequence peptide (CSP) derived from apoA-I, A-IV, and E3, and a real sequence peptide (RSP) corresponding to residues 99−143 of apoA-I (*21*). Such a hysteresis suggests that the thermal unfolding of apolipoproteins on discoidal DMPC complexes is a thermodynamically irreversible transition.

To analyze in greater detail the reversibility of the thermal unfolding of lipid-free and lipid-bound apoA-I, we compared

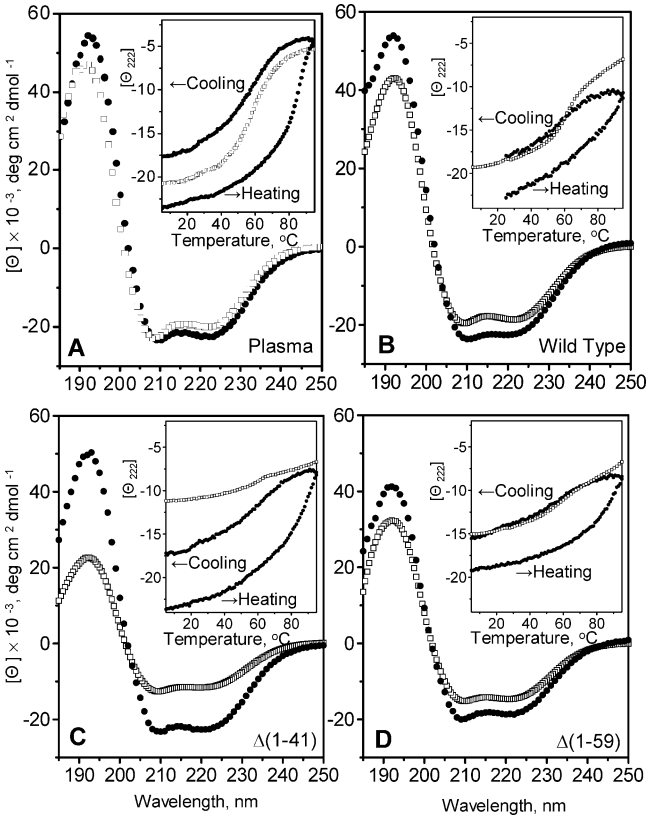

FIGURE 5: Far-UV CD spectra of variant apoA-I forms in lipid-free and -bound states. □: apoA-I in lipid-free state and ●: apoA-I on apoA-I/DMPC complexes. Insets: thermal transition curves of variant apoA-I forms in lipid-free and -bound states recorded at 222 nm. The data are shown in units of $[\theta_{222}] \times 10^{-3}$ deg cm^2 dmol^{-1}. In contrast to lipid-bound proteins (●), the heating curves of lipid-free proteins (□) largely overlap the cooling curves (not shown).

Table 2: Secondary Structure of Variant ApoA-I Forms

	α-helical content (%)[a] at 25 °C			
		DMPC bound		
	lipid-free[b]	before melt	after melt	no. of helical residues increased upon DMPC binding/total residues
plasma	60%	65%	50%	12/243
WT	55%	65%	55%	25/248
Δ(1−41)	40%	65%	48%	51/207
Δ(1−59)	45%	55%	44%	19/189

[a] The α-helical content is the mean value derived from three to five independent measurements of two to three different samples. The error in this estimate is 3%. [b] From ref *15*.

the shapes of the CD melting curves, $\theta_{222}(T)$, that were recorded for plasma apoA-I in solution and on the DMPC disks (Figure 6). The data in Figure 6 were recorded upon heating from 5 to 95 °C followed by cooling to 5 °C at a rate of $\upsilon = 1.0$ K/min. The shape of the thermal unfolding curve, which is another indicator of the transition reversibility, is significantly different for the lipid-free and DMPC-bound apoA-I.

The unfolding curve $[\theta_{222}(T)]$ of lipid-free apoA-I is symmetric and can be approximated by a single sigmoidal function. This symmetry is reflected in the first derivative of the melting data, $d[\theta_{222}(T)]/dT$, that is well-approximated by a single Gaussian function (Figure 6 inset, solid line). The midpoint of the transition, $T_{1/2}$, at which 50% of the total change in the CD amplitude was observed, was about

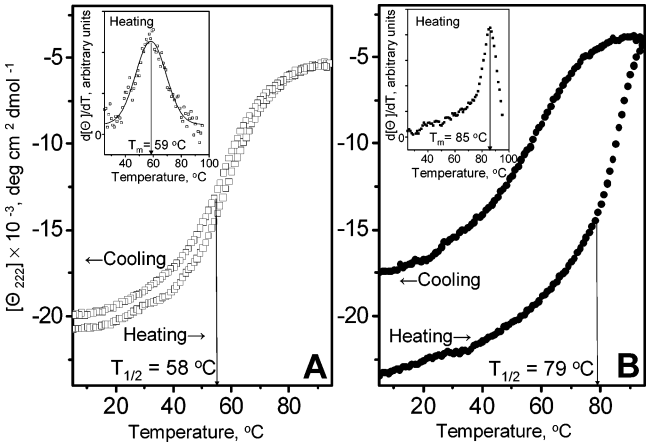

FIGURE 6: Heat unfolding and refolding of plasma apoA-I in the lipid-free state and on apoA-I/DMPC complexes. The thermal transition was monitored by CD at 222 nm upon heating and cooling at a rate $\upsilon = 1.0$ K/min. Arrows indicate the midpoint $T_{1/2}$ of the unfolding transition. (A) Lipid-free plasma apoA-I (□) and (B) ApoA-I/DMPC complexes (●). Insets: first derivative functions $d[\theta_{222}]/dT$ of the heat unfolding curves. The peak positions shown by arrows indicate the apparent melting temperature T_m.

58 °C, in good agreement with the apparent melting temperature $T_m = 59 \pm 1$ °C determined from the peak position in the first derivative function (Figure 6A, inset) and with the value of $T_m = 57 \pm 1$ °C determined by a conventional van't Hoff analysis of apoA-I (*22*). Such an agreement between T_m and $T_{1/2}$ is characteristic of an equilibrium (reversible) thermal transition.

In contrast to free protein, the unfolding curve of apoA-I on apoA-I/DMPC complexes recorded upon heating from 5 to 95 °C at a rate 1.0 K/min was asymmetric. In the heat unfolding process, the CD signal changed more slowly at low temperature and faster (steeper curve) at high temperature. This resulted in a significant difference between the values of $T_{1/2} = 79 \pm 2$ °C and $T_m = 85 \pm 1$ °C (Figure 6B). The first derivative of the melting curve, $d[\theta_{222}(T)]/dT$, was also asymmetric (steeper at high temperatures) and could not be approximated by a single Gaussian function (Figure 6B, inset). Such an asymmetry in the unfolding curve and its first derivative function, along with the presence of the hysteresis, suggests a shift in the population distribution toward the preexisting species, which is characteristic of a slow irreversible transition associated with a high energy barrier.

Scan Rate Effects on the Thermal Transition of Plasma ApoA-I/DMPC Complexes. To analyze the unfolding kinetics of apoA-I/DMPC disks, the thermal unfolding and refolding data $[\theta_{222}(T)]$ were recorded at different heating/cooling rates from 1.0 to 0.067 K/min. The heat unfolding curves showed a progressive low-temperature shift upon reduction in scan rate from 1.0 to 0.067 K/min (Figure 7A), with the reduction in $T_{1/2}$ from 79 °C (at 1.0 K/min) to 68 °C (at 0.067 K/min), and in T_m from about 86 °C to 74 °C. Such a shift indicated a high activation enthalpy of the transition.

The cooling curves (corresponding to the protein refolding) also shifted to lower temperatures upon reduction in the cooling rate. Such a shift may result from the formation of larger and/or multilamellar liposomes at slower heating rates that was observed in similar studies of apoC-I/DMPC disks (*20*). If equilibrium could be attained at slow scan rates, the unfolding and refolding curves would shift toward each other and eventually overlap (reversible unfolding). However, the CD curves in Figure 7A showed an opposite trend (i.e., low-temperature shifts in both heating and cooling curves upon reduction in the scanning rate) resulting in noncoincidence between the heating and the cooling curves at any scan rate. Therefore, the apoA-I thermal unfolding and refolding on the disks is a nonequilibrium transition at any scan rate explored.

The observed scan rate effects on the heating curves of the apoA-I/DMPC disks indicated a high activation energy (enthalpy) E_a for the unfolding transition. The value of E_a was determined from the heating rate dependence of T_m as described in the Materials and Methods. This method was originally proposed by Sanchez-Ruiz (*19*) in the differential scanning calorimetry study of the irreversible thermal denaturation of thermolysin. In our study, the values of T_m at different scan rates υ were determined from the peak positions in the first derivatives of the melting curves in Figure 7A. The plot $\ln(\upsilon/T_m^2)$ versus $(1/T_m)$ was linear (Figure 7B), suggesting a small activation heat capacity. The activation energy E_a calculated from the slope $(-E_a/R)$ of this plot was $E_a = 60 \pm 5$ kcal/mol; the error in this estimate incorporated the fitting errors and the deviations between repetitive experiments. This value of E_a is consistent with the earlier spectroscopic and calorimetric studies of apoA-I/DMPC complexes that indicated large scan rate effects on T_m and suggested a high activation enthalpy $\Delta H^* \approx 40$ kcal/mol for the complex denaturation (*23*, *24*). Our results are also consistent with the heat unfolding studies of apoC-I/DMPC disks showing that the disks are kinetically but not thermodynamically stable (*20*). Interestingly, the activation energy E_a determined in our studies of apoA-I/DMPC complexes ($E_a \sim 60$ kcal/mol) was substantially higher than that of apoC-I/DMPC complexes ($E_a \sim 25$ kcal/mol), which may be due to the larger size of apoA-I molecule (243 aa) as compared to apoC-I (57 aa).

Thermal Unfolding of DMPC Complexes with Wild-Type and N-Terminal Deletion Mutants. Thermal unfolding curves of DMPC complexes with wild type and N-terminal deletion mutants were nearly linear (Figure 5B−D, insets) and did not show a single well-defined peak in the first derivative function, $d[\theta_{222}(T)]/dT$. This precluded the determination of the melting temperature T_m for these protein/lipid complexes. Interestingly, in their lipid-free state, these proteins also showed nearly linear low-cooperative unfolding at pH 7.8 (*15*). Thus, the unfolding cooperativity of these proteins did not substantially increase upon lipid binding.

The limited quantity precluded the analysis of the scan rate effects on the thermal transitions of the mutant apoA-I/DMPC disks. However, the hysteresis in the heat unfolding and refolding of these variant apoA-I forms on DMPC disks observed at a scan rate of $\upsilon = 1.0$ K/min (Figure 5B−D, insets) suggested that the unfolding of these mutant/DMPC complexes was also an irreversible kinetically controlled transition.

DISCUSSION

Terminal Deletion Affects the Lipid-Binding Ability of ApoA-I. Our studies show clear differences in the lipid-binding ability of plasma, wild type, and the terminally

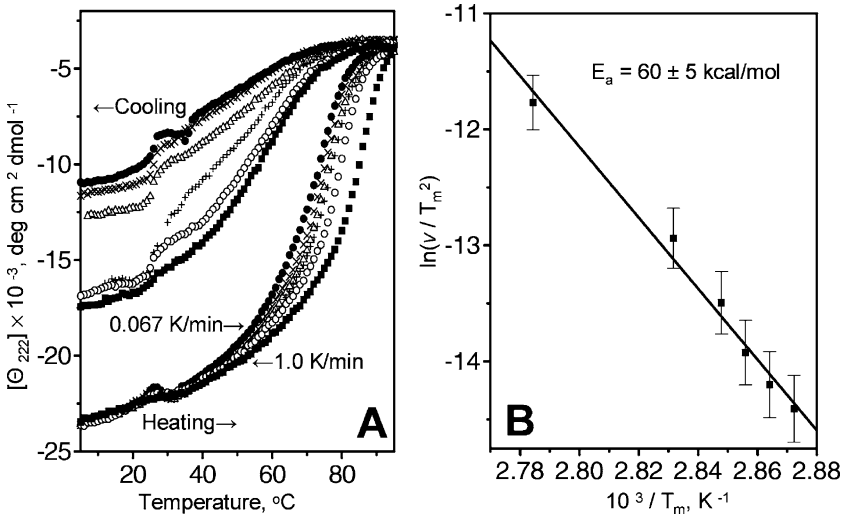

FIGURE 7: Scanning rate effects on the thermal transition of plasma apoA-I on DMPC disks. (A) Thermal unfolding and refolding curves recorded by CD at 222 nm upon heating and cooling from 5 to 85 °C at several constant rates: ■■■ 1.0 K/min, ○○○ 0.3 K/min, +++ 0.17 K/min, △△△ 0.11 K/min, ××× 0.083 K/min, and ●●● 0.067 K/min. (B) Activation energy E_a determined from the scan rate effects on the apparent melting temperature T_m. The error bars represent uncertainty in the T_m determination. Solid line shows linear regression fitting of the data $\ln(v/T_m^2)$ vs $1/T_m$. E_a determined from the slope of this line is 60 ± 5 kcal/mol.

truncated mutants of apoA-I. The plasma and wild-type apoA-I have the highest lipid-binding ability. They clear the turbid DMPC dispersion very quickly, show a major peak for both protein and lipid at a density ~1.10 g/cm^3 after density gradient centrifugation analysis, and exhibit characteristic disk stacks of apoA-I/DMPC complexes in EM micrographs. N-terminal deletion mutants, Δ(1−41) and Δ(1−59), have lower lipid-binding ability, with significantly slower clearance of DMPC liposomes and fewer discoidal complexes observed in EM micrographs. The double deletion mutants, Δ(1−41, 185−243) and Δ(1−59, 185−243), have the poorest lipid-binding ability, with barely detectable apoA-I/DMPC disks in EM micrographs. These results suggest that the N-terminal deletion diminishes the lipid-binding ability of apoA-I, and the C-terminal 185−243 deletion almost completely abolishes the ability of apoA-I to form discoidal complexes with phospholipid. It is possible that the slight differences in lipid binding of the wild-type protein and the plasma apoA-I might, at least in part, result from the presence of the five additional amino acid residues at the N-terminus where the rTEV cleavage site was located (*15*). However, since all the expressed proteins contain these additional residues, comparison of their lipid-binding properties is internally consistent.

Our results agree with the studies of a synthetic peptide that suggest the essential role of the N-terminal residues 44−65 for the lipid-binding properties of apoA-I (*12*, *25*, *26*). A synthetic peptide of residues 1−44 can also bind to DMPC and form disks with density similar to that of plasma apoA-I/DMPC disks (Hongli Zhu and David Atkinson, unpublished data). These results suggest that the N-terminal domain, which is important in the stabilization of the lipid-free protein, may favor lipid binding by maintaining a certain conformation in which the initial lipid-binding sites of the protein are accessible to the lipid (*27*).

Limited proteolysis and deletion mutant studies showed that the C-terminal domain (mainly residues 193−243) plays a key role in the initiation of apoA-I−lipid interactions (*28*−*31*). Studies on apoA-I Nichinan, a naturally occurring human apoA-I mutant with a deletion of Glu235, indicated a substantial reduction in the lipid-binding ability (*11*). The mutation studies on the C-terminal residues 209−243 revealed that large hydrophobic residues (Leu and Phe) are important in the initial lipid binding (*10*). All these results suggest that the C-terminal part is involved in the initial association of apoA-I with phospholipids and in the formation of lipoprotein particles in vivo.

Our studies substantiate the presence of important lipid-binding sites in the C-terminal domain of apoA-I. We also demonstrate that the deletion of only the N-terminal part diminishes but not totally abolishes the ability of apoA-I to bind lipid, suggesting a significant role for the first 41 residues in the lipid-binding process.

Secondary Structure Changes in Variant ApoA-I Induced by DMPC. The α-helical content of all variant apoA-I forms increased upon DMPC binding, with a 5% increase in plasma, 10% increase in wild type and Δ(1−59), and nearly 25% increase in Δ(1−41). Secondary structure models for these apoA-I mutants in their lipid-free conformation were proposed in our earlier work (*15*). Residues 42−59 were inferred to be unfolded in Δ(1−41) in solution. Therefore, the large increase in α-helical content in Δ(1−41) but not in Δ(1−59) suggests that the 42−59 segment may fold into a helical conformation upon association with DMPC. Similarly, the C-terminal region 176−243, which was inferred to be disordered in the lipid-free state, may fold into a helical structure upon lipid binding. Furthermore, the increase in the number of helical residues upon DMPC binding is much larger in Δ(1−41) (51 residues) than in Δ(1−59) (19 residues) (Table 2). This indicates the presence of potential lipid-binding or lipid-binding assisting sites in this 42−59 segment and suggests that a structured state of a 42−59 segment may facilitate the folding and lipid binding of the central and C-terminal region of apoA-I.

pH Effects on the Lipid-Binding Ability and the Secondary Structure of the Variant ApoA-I Forms in the ApoA-I/DMPC Complexes. Our studies suggest that the wild type and mutant Δ(1−41) had increased lipid-binding ability upon the reduction in pH from 7.8 to 4.7. Indeed, density gradient centrifugation analysis of these proteins incubated with

DMPC showed better-defined and higher amplitude peaks for both the protein and the lipid at a density ~1.10 g/cm^3 corresponding to the density of the apoA-I/DMPC disks (Figure 3). Interestingly, no significant pH-dependent changes in the lipid-binding ability were observed for the mutants Δ(1−59), Δ(1−41, 185−243), and Δ(1−59, 185−243). For the double deletion mutants (data not shown), this is easy to understand since these proteins hardly bind to DMPC because of the deletion of the C-terminus that may contain the initial lipid-binding sites. For Δ(1−59), it is possible that the deletion of 1−59 residues removed a part of another essential lipid-binding site encompassing residues 44−65, so the pH effects were not observed due to the impaired lipid-binding ability of this mutant.

The secondary structure of the variant forms of apoA-I in the lipid-bound state is mainly α-helical, as indicated by their far-UV CD spectra. Studies of pH effects on the secondary structure of apoA-I in complex with DMPC showed that the α-helical content of plasma and wild-type apoA-I did not change significantly upon the reduction in pH from 7.8 to 4.7. In contrast, the mutants Δ(1−41) and Δ(1−59) in complex with DMPC showed a ~10% increase in their α-helical content at pH 4.7, similar to that observed in lipid-free proteins upon reduction in pH. This suggests that the pH of the environment may have a significant impact on the secondary structure of the apoA-I both in lipid-free and in lipid-bound states. The thermal unfolding of the variant complexes at low pH suggested that their unfolding cooperativity increased, as indicated by more sigmoidal unfolding curves for the lipid-bound as compared to lipid-free proteins. The unfolding curves at low pH also showed hysteresis and suggested a kinetic barrier during the transition (data not shown). Since the pI of plasma apoA-I is around 5.2, the net charge of the protein changed sign in our experiments in which the pH was reduced from 7.8 to 4.7. This clearly had an impact on the ability of apoA-I to form stable discoidal complexes with phospholipids and the conformation and the stability of the complexes.

The NMR structure of a peptide fragment of apoA-I (residues 166−185) on SDS or dodecylphosphocholine (DPC) micelles also showed significant pH-dependent structural changes between pH 6.6 and 3.7 (*32*). NMR spectra of these peptide−micelle complexes indicate a more extensive α-helical structure in the N-terminus at lower pH. These NMR results are consistent with our CD spectroscopic data showing that a reduction in pH in the acidic region may lead to an increase in the apolipoprotein α-helical content in the protein/lipid complexes.

In summary, reduction in pH from 7.8 to 4.7 leads to an increase in the α-helical content and the lipid-binding ability of apoA-I and some of its terminally truncated mutant forms. This clearly indicates the importance of the electrostatic interactions for the lipid binding and the discoidal complex formation by apoA-I.

Kinetically Controlled Thermal Unfolding of ApoA-I on ApoA-I/DMPC Complexes. The heat unfolding and refolding curves of variant apoA-I forms on apoA-I/DMPC complexes show hysteresis. Moreover, the unfolding curves of complexes with plasma apoA-I show a progressive low-temperature shift upon reduction in the heating rate. This indicates a slow nonequilibrium thermal transition associated with a high activation energy. Our results corroborate earlier reports of irreversible unfolding of apoA-I/DMPC disks that revealed a kinetically controlled thermal and chemical transition (*23*, *24*, *33*). The activation energy determined in our study of plasma apoA-I/DMPC disks, $E_a = 60 \pm 5$ kcal/mol, indicates a major enthalpic contribution to the free-energy barrier for the thermal transition. The high activation energy of disk denaturation was also observed in other apolipoprotein−DMPC complexes, such as apoC-I/DMPC (*20*), CSP/DMPC, and RSP/DPMC disks (*21*). These observations suggest that the kinetic mechanism may be the general paradigm for the stabilization of discoidal lipoproteins, including nascent HDL particles that also contain phosphatidylcholines as their major lipid component. The slow kinetics of apolipoprotein unfolding on the disks may be physiologically important. It may help the protein/lipid complexes to maintain their structural integrity and function regardless of their low thermodynamic stability.

ACKNOWLEDGMENT

We thank Drs. Vassilis Zannis and Tong Liu for the collaboration in the apoA-I expression system. Cheryl England and Dr. Haya Herscovitz have offered much help in the ultracentrifugation experiments. We are very grateful to Don Gantz for his help in EM experiments, and we also thank Dr. Yang Chao for many helpful discussions.

REFERENCES

1. Atkinson, D., and Small, D. M. (1986) Recombinant lipoproteins: Implications for structure and assembly of native lipoproteins, *Annu. Rev. Biophys. Biophys. Chem. 15*, 403−456.
2. Miller, N. E. (1987) Associations of high-density lipoprotein subclasses and apolipoproteins with ischemic heart disease and coronary atherosclerosis, *Am. Heart J. 113*, 589−597.
3. Small, D. M. (1992) Structure and Metabolism of the Plasma Lipoproteins, in *Current Issues in Endocrinology and Metabolism: Plasma Lipoproteins and Coronary Artery Disease* (Kreisberg, R. A., and Segrest, J. P., Eds.) pp 57−91, Blackwell Scientific Publications, Boston, MA.
4. Attie, A. D., Kastelein, J. P., and Hayden, M. R. (2001) Pivotal role of ABCA1 in reverse cholesterol transport influencing HDL levels and susceptibility to atherosclerosis, *J. Lipid Res. 42*, 1717−1726.
5. Nolte, R. T., and Atkinson, D. (1992) Conformational analysis of apolipoprotein A-I and E-3 based on primary sequence and circular dichroism, *Biophys. J. 63*, 1221−1239.
6. Jonas, A., Kezdy, K. E., and Wald, J. H. (1989) Defined apolipoprotein A-I conformations in reconstituted high-density lipoprotein discs, *J. Biol. Chem. 264*, 4818−4824.
7. Jonas, A., Wald, J. H., Toohill, K. L., Krul, E. S., and Kezdy, K. E. (1990) Apolipoprotein A-I structure and lipid properties in homogeneous, reconstituted spherical, and discoidal high-density lipoproteins, *J. Biol. Chem. 265*, 22123−22129.
8. Jonas, A. (1986) Reconstitution of high-density lipoproteins, *Methods Enzymol. 128*, 553−582.
9. Brouillette, C. G., Anantharamaiah, G. M., Engler, J. A., and Borhani, D. W. (2001) Structural models of human apolipoprotein A-I: a critical analysis and review, *Biochim. Biophys. Acta 1531*, 4−46.
10. Laccotripe, M., Makrides, S. C., Jonas, A., and Zannis, V. I. (1997) The carboxyl-terminal hydrophobic residues of apolipoprotein A-I affect its rate of phospholipid binding and its association with high-density lipoprotein, *J. Biol. Chem. 279*, 17511−17522.
11. Huang, W., Sasaki, J., Matsunaga, A., Han, H., Li, W., Koga, T., Kugi, M., Ando, S., and Arakawa, K. (2000) A single amino acid deletion in the carboxyl terminal of apolipoprotein A-I impairs lipid binding and cellular interaction, *Arterioscler., Thromb., Vasc. Biol. 20*, 210−216.
12. Palgunachari, M. N., Mishra, V. K., Lund-Katz, S., Phillips, M. C., Adeyeye, S. O., Alluri, A., Anantharamaiah, G. M., and

Segrest, J. P. (1996) Only the two end helices of eight tandem amphipathic helical domains of human apoA-I have significant lipid affinity implications for HDL assembly, *Arterioscler., Thromb., Vasc. Biol. 16*, 328−338.
13. Rogers, D. P., Roberts, L. M., Lebowitz, J., Datta, G., Anantharamaiah, G. M., Engler, J. A., and Brouillette, C. G. (1998) The lipid-free structure of apolipoprotein A-I: Effects of amino-terminal deletions, *Biochemistry 37*, 11714−11725.
14. McManus, D. C., Scott, B. R., Frank, P. G., Franklin, V., Schultz, J. R., and Marcel, Y. L. (2000) Distinct central amphipathic α-helices in apolipoprotein A-I contribute to the in vivo maturation of high-density lipoprotein by either activating lecithin-cholesterol acyltransferase or binding lipids, *J. Biol. Chem. 275*, 5043−5051.
15. Fang, Y., Gursky, O., and Atkinson, D. (2003) Structural studies of N- and C-terminally truncated human apolipoprotein A-I, *Biochemistry 42*, 6881−6890.
16. Gorshkova, I. N., Liu, T., Zannis, V. I., and Atkinson, D. (2002) Lipid-free structure and stability of apolipoprotein A-I: Probing the central region by mutation, *Biochemistry 41*, 10529−10539.
17. Lowry, O. H., Rosebrough, N. J., Farr, A. L., and Randall, R. J. (1951) Protein measurement with the Folin Phenol reagent, *J. Biol. Chem. 193*, 265−275.
18. John, D. M., and Weeks, K. M. (2000) van't Hoff enthalpies without baselines, *Protein Sci. 9*, 1416−1419.
19. Sanchez-Ruiz, J. M., Lopez-Lancomba, J. L., Cortijo, M., and Mateo, P. L. (1988) Differential scanning calorimetry of irreversible thermal denaturation of thermolysin, *Biochemistry 27*, 1648−1652.
20. Gursky, O., Ranjana, and Gantz, D. (2002) Complex of human apolipoprotein C-1 with phospholipids: Thermodynamic or kinetic stability? *Biochemistry 41*, 7373−7384.
21. Chao, Y. (2002) Conformational Studies of a Concensus Sequence Peptide (CSP) and a Real Sequence Peptide (RSP) of Apolipoproteins by Circular Dichroism and X-ray Crystallography, Ph.D. Thesis, Department of Biophysics, Boston University School of Medicine, Boston, MA.
22. Gursky, O., and Atkinson, D. (1996) Thermal unfolding of human high-density apolipoprotein A-I: Implication for a lipid-free molten globular state, *Proc. Natl. Acad. Sci. U.S.A. 93*, 2991−2995.
23. Surewicz, W. K., Epand, R. M., Pownall, H. J., and Hui, S.-W. (1986) Human apolipoprotein A-I forms thermally stable complexes with anionic but not zwitterionic phospholipids, *J. Biol. Chem. 261*, 16191−16197.
24. Epand, R. M. (1982) The apparent preferential interaction of human plasma high-density apolipoprotein A-I with gel-state phospholipids, *Biochim. Biophys. Acta 712*, 146−151.
25. Mishra, V. K., Palgunachari, M. N., Datta, G., Phillips, M. C., Lund-Katz, S., Adeyeye, S. O., Segrest, J. P., and Anantharamaiah, G. M. (1998) Studies of synthetic peptides of human apolipoprotein A-I containing tandem amphipathic α-helices, *Biochemistry 37*, 10313−10324.
26. Gillotte, K. L., Zaiou, M., Lund-Katz, S., Anantharamaiah, G. M., Holvoet, P., Dhoest, A., Palgunachari, M. N., Segrest, J. P., Weisgraber, K. H., Rothblat, G. H., and Phillips. M. C (1999) Apolipoprotein-mediated plasma membrane microsolubilization. Role of lipid affinity and membrane penetration in the efflux of cellular cholesterol and phospholipids, *J. Biol. Chem. 274*, 2021−2028.
27. Frank, P. G., and Marcel, Y. L. (2000) Apolipoprotein A-I: structure−function relationships, *J. Lipid Res. 41*, 853−872.
28. Ji, Y., and Jonas, A. (1995) Properties of an N-terminal proteolytic fragment of apolipoprotein A-I in solution and in reconstituted high-density lipoproteins, *J. Biol. Chem. 270*, 11290−11297.
29. Rogers, D. P., Roberts, L. M., Lebowitz, J., Engler, J. A., and Brouillette, C. G. (1998b) Structural analysis of apolipoprotein A-I: Effects of amino- and carboxy-terminal deletions on the lipid-free structure, *Biochemistry 37*, 945−955.
30. Burgess, J. W., Frank, P. G., Franklin, V., Liang, P., McManus, D. C., Desforges, M., Rassart, E., and Marcel, Y. L. (1999) Deletion of the C-terminal domain of apolipoprotein A-I impairs cell surface binding and lipid efflux in macrophage, *Biochemistry 38*, 14524−14533.
31. Saito, H., Dhanasekaran, P., Nguyen, D., Holvoet, P., Lund-Katz, S., and Phillips, M. C. (2003) Domain structure and lipid interaction in human apolipoproteins A-I and E, a general model, *J. Biol. Chem. 278*, 23227−23232.
32. Wang, G., Treleaven, W. D., and Cushley, R. J. (1996) Conformation of human serum apolipoprotein A-I (166−185) in the presence of sodium dodecyl sulfate or dodecylphosphocholine by ^{1}H NMR and CD: Evidence for specific peptide−SDS interaction, *Biochim. Biophys. Acta 1301*, 174−184.
33. Reijingoud, D.-J., and Phillips, M. C. (1982) Mechanism of dissociation of human apolipoprotein A-I from complexes with dimyristoylphosphatidylcholine as studied by guanidine hydrochloride denaturation, *Biochemistry 21*, 2969−2976.

BI0354031